The PS/PDI: a high accuracy development tool for diffraction limited short-wavelength optics

Patrick Naulleau[a], Kenneth A. Goldberg[a], Sang H. Lee[a,b], Chang Chang[a,b], Phillip Batson[a], David Attwood[a,b], and Jeffrey Bokor[a,b]

[a] *Center for X-Ray Optics, Lawrence Berkeley National Laboratory, Berkeley, CA 94720*
[b] *EECS Department, University of California, Berkeley, CA 94720*

Abstract. The extreme ultraviolet (EUV) phase-shifting point diffraction interferometer (PS/PDI) was developed and implemented at Lawrence Berkeley National Laboratory to meet the significant measurement challenge of characterizing EUV projection lithography optics. The PS/PDI has been in continuous use and under ongoing development since 1996. This unique and flexible tool is applicable to any imaging system with real conjugate points, including Schwarschild objectives, Fresnel zone plates, and Kirkpatrick-Baez systems. Here we describe recent improvements made to the interferometer, and we summarize metrology results from state-of-the-art 10×-reduction EUV Schwarschild objective.

INTRODUCTION

The quest to develop extreme ultraviolet (EUV) optics for use in next-generation projection lithography systems providing sub-100-nm resolution has led to various innovations in EUV wavefront metrology,[1,2] including the development of the EUV phase-shifting point diffraction interferometer (PS/PDI).[3-5] Not being limited to EUV lithographic systems, the metrology capabilities of the PS/PDI are directly applicable to the development of high-resolution X-ray microscopy tools.

The PS/PDI is a diffraction-class interferometer,[6-8] in which the illumination and reference waves are created by diffraction from small apertures. Furthermore, a diffraction grating is used as the beam-splitting and phase-shifting element. This diffraction configuration allows the PS/PDI to attain high reference-wavefront accuracy which has recently been measured to be better than $\lambda_{EUV}/350$ (0.4 Å) within a numerical aperture (NA) of 0.082.[9]

The PS/PDI is a flexible, system-level tool that may be applied to characterizing any imaging system with real conjugate points. Such systems, commonplace in X-ray microscopy, include Schwarschild objectives, Fresnel zone plates, and Kirkpatrick-Baez optics. Another advantage of the PS/PDI is that its diffraction characteristics, in principle, allow it to be implemented at virtually any wavelength. Here we describe the PS/PDI as implemented to test EUV 10×-reduction Schwarschild systems.

When characterizing imaging systems, it is important to consider flare in addition to wavefront error. Flare is the *halo* of light surrounding the optical system point-

CP507, *X-Ray Microscopy: Proceedings of the Sixth International Conference,*
edited by W. Meyer-Ilse, T. Warwick, and D. Attwood

spread function (PSF) and is caused by roughness of the optical components. While conventional wavefront errors directly lead to a loss of resolution, flare negatively affects the image contrast. In order to enable direct measurement of flare using the PS/PDI, the PS/PDI has recently been modified to support a greatly extended spatial-frequency measurement range.[10] This new capability also enables the PS/PDI to be used to qualify profilometry- and scatterometry-based flare measurement techniques.[11]

DESCRIPTION OF THE PS/PDI

The PS/PDI is briefly described here; more complete descriptions have been previously published.[3-5] The PS/PDI is a variation of the conventional point diffraction interferometer[6,7] in which a transmission grating is added to improve the optical throughput of the system and to add phase-shifting capability. In the PS/PDI (Fig. 1), the optical system under test is coherently illuminated by a spherical wave generated by diffraction from a pinhole placed in the object plane. To guarantee the quality of the illumination, the pinhole diameter is chosen to be smaller than the resolution limit of the optical system. A grating placed either before or after the optic is used to split the illuminating beam, creating the requisite test and reference beams. A mask (the *PS/PDI mask* in Fig. 1) is placed in the image plane of the optic to block unwanted diffracted orders generated by the grating. The mask also serves to spatially filter the reference beam using a second pinhole (the *reference pinhole*), thereby, removing the aberrations imparted by the optical system. The test beam, which also contains the aberrations imparted by the optical system, is largely undisturbed by the image-plane mask: it passes through a window that is large relative to the diameter of the optical system PSF. The test and reference beams propagate to the detector where they overlap to create an interference pattern. The recorded interferogram yields information on the deviation of the test beam from the nominally spherical reference beam.

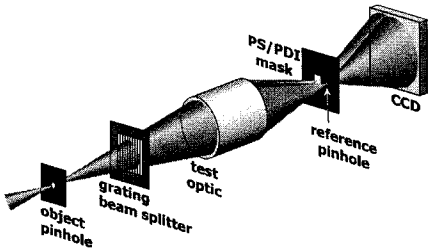

FIGURE 1. Schematic of the phase-shifting point diffraction interferometer (PS/PDI).

CHARACTERIZING ACCURACY

Significant effort has been directed toward characterizing the accuracy of the PS/PDI.[9] The two primary sources of measurement error limiting its accuracy are reference-wave imperfections and systematic effects that arise from the geometry of the system. Noting that the systematic geometric effects can be removed, provided they can be measured, the accuracy of the PS/PDI is typically limited by the reference-pinhole-induced errors.

In order to characterize the errors described above, and hence calibrate the PS/PDI, null tests have been performed. Analogous to Young's two-slit experiment, the null

test is implemented by replacing the image-plane window with a pinhole. In this test, two reference waves are generated by diffraction from the image-plane mask, creating a null-test interferogram (Fig. 2). Aberrations calculated from the null-test interferogram quantify the systematic and random errors in the interferometer.

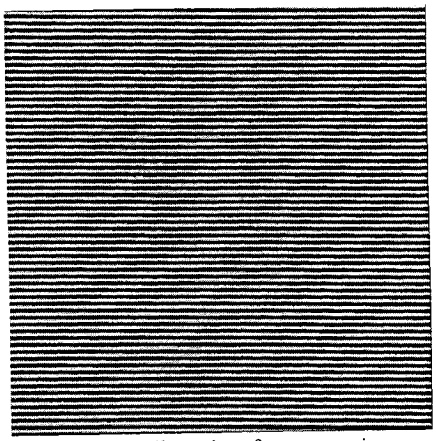

FIGURE 2. Null-test interferogram using 100-nm pinholes (λ = 13.5 nm).

Implementation of this test shows that the primary error results from the hyperbolic fringe pattern produced by the two, laterally displaced, nominally spherical waves. Because this error is easily measured and subtracted during analysis,[5] we consider the reference-wavefront-limited accuracy to be the residual error after its removal. Table 1 enumerates the measured accuracy as a function of pinhole size over a NA of 0.082. The image-side NA of the optic used for this test was 0.08. As expected, the reference-wavefront accuracy improves with a reduction in pinhole size, and a resultant improvement in spatial filtering.

TABLE 1. Reference wave rms accuracy as a function of null-mask pinhole size.

Pinhole Size (nm)	Systematic-error-limited rms Accuracy (waves)
140	0.012 ± 0.001 (λ/83)
120	0.010 ± 0.001 (λ/100)
100	0.0041 ± 0.0003 (λ/244)
80	0.0028 ± 0.0001 (λ/357)

The measurements described here were performed using an undulator beamline[12] at the Advanced Light Source synchrotron radiation facility at Lawrence Berkeley National Laboratory. The beamline provides a tunable source of EUV radiation with a coherence area that is significantly larger than the 0.75-μm diameter object pinhole.[12]

CHARACTERIZING AND ALIGNING EUV OBJECTIVES

During the past year, three newly fabricated 10×-reduction EUV Schwarzschild objectives have been characterized with the EUV PS/PDI. Furthermore, two of the objectives underwent at-wavelength alignment, significantly improving the system wavefronts.[13] All three cameras were fabricated to the same optical design specifications and were built within the past two years. The optics have an image-side NA of 0.088 and utilize molybdenum/silicon multilayer coatings designed for peak reflectivity at 13.4 nm wavelength.

Figure 3 shows the PS/PDI measured wavefronts along with the rms (σ) and peak-to-valley (PV) wavefront error magnitudes within the full 0.088 NA. EUV alignment was performed on objectives **B2** and **A**. These results demonstrate that the PS/PDI is well suited to characterizing and, more importantly, optimizing short-wavelength high-resolution optical systems.

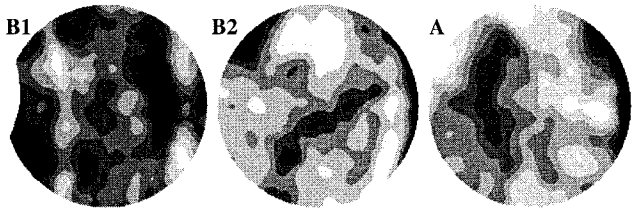

FIGURE 3. PS/PDI-measured wavefronts of three recently fabricated 10×-reduction EUV (λ=13.4 nm) Schwarzschild objectives with an image side NA of 0.088. The wavefront statistics are based on 37-term Zernike polynomial fitting. The displayed wavefronts, however, include higher spatial-frequency features.

MEASURING FLARE

The original design of the PS/PDI was directed towards high-accuracy wavefront characterization. For lithographic printing, however, it is equally important to consider flare. The capabilities of the PS/PDI have recently been extended, allowing it to measure both wavefront and flare simultaneously.[10] Flare may be characterized by recording an extended-field image of the PSF. Noting that the PS/PDI can be viewed as producing an off-axis Fourier-transform hologram of the PSF, it is well suited to measuring flare. From this point of view it is evident that the area over which the flare can be measured in the image plane is simply the area of the test window through which the PSF is effectively viewed. Using elongated windows it is possible to characterize the flare over significant distances in the image plane.[10]

The PS/PDI-based flare measurement technique has been demonstrated[10] using the **B1** EUV objective described above. This optical system developed to meet a flare specification of less than 5% in a 4-μm line. The measurements were performed using 30×3-μm test windows. The narrow window size in the direction of the beam separation is necessary to meet the beam isolation requirements imposed by off-axis holography.[14]

Figure 4 shows a logarithmically scaled image of the holographically reconstructed image of the PSF with flare. The image contains the customary twin images and intermodulation image.[14] Because the reconstructed image is as viewed through the image-plane window, we simultaneously get an image of the window itself. The bars seen in Fig. 4 are support features added to the window to prevent the thin, open-stenciled membrane from rupturing. The small (0.3-μm wide) protrusions in the center window portion are alignment aids. We note that the resolution in the reconstruction is determined by the reference pinhole size, which in this case is approximately 100 nm.

From the measured PSF, the normalized scatter-energy density as a function of radial distance from the PSF peak can be found (Fig. 5). The imperfect Airy lobes are caused by aberrations in the optic (figure error). To predict the flare in a typical imaging situation, the scatter-energy density must be known over the full radial extent of the field. For the optics considered here the field size is 250-μm radius in the image plane. The extended-range data can be obtained by extrapolation of the PS/PDI data or

by use of data derived from profilometry performed on the individual substrates.[11] In order to avoid possible extrapolation errors, we choose the latter. The plot in Fig. 5 shows an overlay of the scatter-energy density predicted from profilometry and the PS/PDI measurement. The two measurement methods overlap in the radial range from 1 to 16 μm where good agreement is evident. Considering an isolated, dark 4-μm line in a 250-μm-radius bright field, the flare is calculated to be (3.9±0.1)%. The flare value predicted by profilometry alone is (4.0±0.1)%.[11]

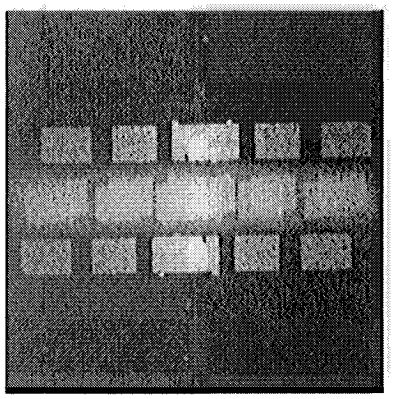

FIGURE 4. Holographically reconstructed point-spread function with flare. Image has been logarithmically scaled for display.

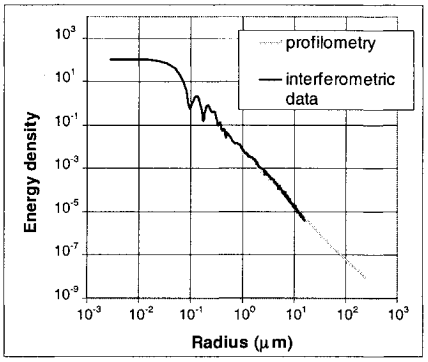

FIGURE 5. Comparison of the scatter-energy density as a function of radial separation from the PSF peak determined by the PS/PDI- and profilometry-based methods respectively.

CONCLUSION

A high accuracy PS/PDI, capable of characterizing both wavefront and flare, has been developed. This versatile diffractive interferometer may be implemented at virtually any wavelength to test a wide range of imaging systems characterized by real conjugate points. As implemented to test 10× Schwarschild objectives, the PS/PDI has been demonstrated to have a reference wavefront accuracy of better than λ/350 (0.4 nm) and has been used to align several lithographic-quality systems. A second implementation of the PS/PDI is currently being developed to test high-resolution Fresnel zone plates to be used in soft X-ray microscopy applications.

ACKNOWLEDGEMENTS

The authors are greatly indebted to Hector Medecki and Edita Tejnil for their pivotal roles in the early development of the PS/PDI. We are also grateful to Erik Anderson for nanofabrication of pinholes and windows, and to members of the CXRO staff, including Bill Bates, Rene Delano, Keith Jackson, Gideon Jones, Drew Kemp, David Richardson, and Senajith Rekewa for facilitating this research. Special thanks are due to Paul Denham for expert assistance with experimental control systems. This

research was supported by the Extreme Ultraviolet Limited Liability Company, the Semiconductor Research Corporation, DARPA Advanced Lithography Program, and the Department of Energy Office of Basic Energy Science.

REFERENCES

1. J. E. Bjorkholm, A. A. MacDowell, O. R. Wood II, Z. Tan, B. LaFontaine, and D. M. Tennant, "Phase-measuring interferometry using extreme ultraviolet radiation," *J. Vac. Sci. & Technol. B* **13**, 2919-2922 (1995).

2. A. K. Ray-Chaudhuri, W. Ng, F. Cerrina, Z. Tan, J. Bjorkholm, D. Tennant, and S. J. Spector, "Alignment of a multilayer-coated imaging system using extreme ultraviolet Foucault and Ronchi interferometric testing," *J. Vac. Sci. Technol. B* **13**, 3089-3093 (1995).

3. H. Medecki, E. Tejnil, K. A. Goldberg, and J. Bokor, "Phase-shifting point diffraction interferometer," *Opt. Lett.* **21**, 1526-1528 (1996).

4. E. Tejnil, K. A. Goldberg, S. H. Lee, H. Medecki, P. J. Batson, P. E. Denham, A. A. MacDowell, J. Bokor, and D. Attwood, "At-wavelength interferometry for EUV lithography," *J. Vac. Sci. & Technol. B* **15**, 2455-2461 (1997).

5. K. A. Goldberg, "Extreme Ultraviolet Interferometry," Ph.D. dissertation (University of California, Berkeley, 1997).

6. W. Linnik, "A simple interferometer to test optical systems," *Proceedings of the Academy of Science of the USSR* **1**, 210-212 (1933).

7. R. N. Smartt and W. H. Steel, "Theory and application of point-diffraction interferometers," *Jap. J. Appl. Phys.* **14**, Suppl.14-1, 351-356 (1975).

8. G. E. Sommargren, "Phase shifting diffraction interferometry for measuring extreme ultraviolet optics," OSA Trends in Optics and Photonics Vol. 4, *Extreme Ultraviolet Lithography*, G. D. Kubiak and D. R. Kania, eds. (Optical Society of America, Washington, DC 1996), pp. 108-112.

9. P. Naulleau, K. A. Goldberg, S. Lee, C. Chang, D. Attwood, and J. Bokor, "The EUV phase-shifting point diffraction interferometer: a sub-angstrom reference-wave accuracy wavefront metrology tool," *Appl. Opt.,* to be published (1999).

10. P. Naulleau, K. A. Goldberg, E. Gullikson, and J. Bokor, "Interferometric at-wavelength flare characterization of EUV optical systems," *J. Vac. Sci. & Technol. B*, to be published (1999).

11. E. Gullikson, S. Baker, J. Bjorkholm, J. Bokor, K. Goldberg, J. Goldsmith, C. Montcalm, P. Naulleau, E. Spiller, D. Stearns, J. Taylor, and J. Underwood, "EUV scattering and flare from 10× projection cameras," in *Emerging Lithographic Technologies III*, Y. Vladimirski, ed., Proc. SPIE, **3676**, 717-723 (1999).

12. D. Attwood, P. Naulleau, K. Goldberg, E. Tejnil, C. Chang, R. Beguiristain, P. Batson, J. Bokor, E. Gullikson, M. Koike, H. Medecki, and J. Underwood, "Tunable coherent radiation in the soft X-ray and extreme ultraviolet spectral regions," *IEEE J. Quantum Electron,* **35**, 709-720 (1999).

13. K. A. Goldberg, P. Naulleau, and J. Bokor, "EUV interferometric measurements of diffraction-limited optics," *submitted to J. Vac. Sci. & Technol. B* (6/99).

14. E. N. Leith and J. Upatnieks, "Reconstructed wavefronts and communication theory," *J. Opt. Soc. Am.*, **52**, 1123-1130 (1962).